European Journal of Radiology Open 8 (2021) 100375

Contents lists available at ScienceDirect

European Journal of Radiology Open

journal homepage: www.elsevier.com/locate/ejro

Original Article

Prediction of treatment response to transarterial radioembolization of liver metastases: Radiomics analysis of pre-treatment cone-beam CT: A proof of concept study

Adrian Kobe [a,*], Juliana Zgraggen [a], Florian Messmer [a], Gilbert Puippe [a], Thomas Sartoretti [a], Hatem Alkadhi [a], Thomas Pfammatter [a], Manoj Mannil [a,b]

[a] Institute of Diagnostic and Interventional Radiology, University Hospital Zurich, University of Zurich, Zurich, Switzerland
[b] Clinic of Radiology, University Hospital Münster, University of Münster, Münster, Germany

ARTICLE INFO

Keywords:
Radiomics
Transarterial radioembolization
Machine learning
Cone-Beam CT

ABSTRACT

Purpose: To investigate the potential of texture analysis and machine learning to predict treatment response to transarterial radioembolization (TARE) on pre-interventional cone-beam computed tomography (CBCT) images in patients with liver metastases.

Materials and Methods: In this IRB-approved retrospective single-center study 36 patients with a total of 104 liver metastases (56 % male, mean age 61.1 ± 13 years) underwent CBCT prior to TARE and follow-up imaging 6 months after therapy. Treatment response was evaluated according to RECIST version 1.1 and dichotomized into disease control (partial response/stable disease) versus disease progression (progressive disease). After target lesion segmentation, 104 radiomics features corresponding to seven different feature classes were extracted with the pyRadiomics package. After dimension reduction machine learning classifications were performed on a custom artificial neural network (ANN). Ten-fold cross validation on a previously unseen test data set was performed.

Results: The average administered cumulative activity from TARE was 1.6 Gbq (± 0.5 Gbq). At a mean follow-up of 5.9 ± 0.8 months disease control was achieved in 82 % of metastases. After dimension reduction, 15 of 104 (15 %) texture analysis features remained for further analysis. On a previously unseen set of liver metastases the Multilayer Perceptron ANN yielded a sensitivity of 94.2 %, specificity of 67.7 % and an area-under-the receiver operating characteristics curve of 0.85.

Conclusion: Our study indicates that texture analysis-based machine learning may has potential to predict treatment response to TARE using pre-treatment CBCT images of patients with liver metastases with high accuracy.

1. Introduction

Transarterial radioembolization (TARE) represents a valuable treatment option in unresectable metastatic liver disease, especially with liver-dominant tumor burden [1]. In TARE, Yttrium-90-microspheres (^{90}Y-microspheres) are applied via a catheter into the hepatic artery leading to an accumulation in liver metastases with resulting radiation-induced cell death [2]. As TARE is a costly and highly demanding therapy requiring a multi-disciplinary team including interventional radiologists, oncologists and nuclear medicine specialists, careful patient selection is crucial.

Previous studies have investigated the value of pre-treatment

Abbreviations: ^{99m}Tc-MAA, ^{99m}technetium labelled macroaggregated albumin; ^{90}Y-microspheres, Yttrium-90-microspheres; ANN, Artificial neural network; CBCT, Cone-beam Computed Tomography; CR, Complete response; CT, Computed tomography; DICOM, Digital Imaging and Communications in Medicine; GLCM, Gray-level co-occurrence matrix; GLDM, Gray-level dependence matrix; GLRLM, Gray-level run length matrix; GLSZM, Gray-level size zone matrix; ICC, Intraclass-correlation coefficient; MR, Magnetic resonance; NGTDM, Neighboring gray tone difference matrix; PD, Progressive disease; PET, Positron emission tomography; PR, Partial response; SD, Stable disease; TACE, Transarterial chemoembolization; TARE, Transarterial radioembolization.

* Corresponding author at: Institute of Diagnostic and Interventional Radiology, University Hospital Zurich, Rämistrasse 100, CH-8091, Zurich, Switzerland.
E-mail address: adrian.kobe@usz.ch (A. Kobe).

https://doi.org/10.1016/j.ejro.2021.100375
Received 12 April 2021; Received in revised form 23 August 2021; Accepted 25 August 2021
Available online 30 August 2021

imaging for the prediction of tumor response after TARE. Consistent with the idea of higher ^{90}Y-microspheres accumulation in hypervascular metastases, some studies showed a favorable outcome of patients having liver metastases showing high arterial perfusion as quantified in an absolute way with computed tomography (CT) perfusion [3,4]. In contrast, another study [5] found no difference in survival after TARE between metastases classified as either hypo- or hypervascular on pre-treatment imaging based on a subjective and purely qualitative grading system for tumor vascularity. In addition, the pattern of ^{99m}technetium labelled macroaggregated albumin (^{99m}Tc-MAA) uptake in liver metastases failed to predict tumor response after TARE [6,7].

Radiomics is an emerging field in medical imaging enabling the objective assessment of tumor heterogeneity by extracting quantitative imaging features which are imperceptible to the human eye [8]. As tumor heterogeneity plays a crucial role in tumor growth and metastases, several recent studies focused on radiomic feature-based texture analysis of tumors showing that texture analysis was able to predict treatment response and prognosis using imaging data from CT, magnetic resonance (MR) imaging and positron emission tomography (PET) in several entities [9–11]. The application of texture analysis and machine learning in interventional oncology have been studied in patients who underwent transarterial chemoembolization (TACE) for hepatocellular carcinoma with promising results [12–15], and one study applied texture analysis to pre-TARE CT images in patients with cholangiocarcinoma [16].

The purpose of this study was to investigate the potential of texture analysis and machine learning to predict treatment response to TARE on pre-interventional cone-beam CT (CBCT) images in patients with liver metastases.

2. Materials and methods

This retrospective study was approved by the local ethics committee. Written informed consent requirement was waived.

2.1. Patients

Between January 2010 and May 2018, a total of 214 patients with liver metastases underwent TARE in our single tertiary referral center. 178 patients were excluded because of missing or incomplete imaging follow-up six months after TARE. Thus, the final study population consisted of 36 patients with a total of 104 analyzed liver metastases (55.6 % male, mean age 61.1 ± 13 years), who underwent CBCT prior to TARE and follow-up imaging 6 months after therapy. Table 1 summarizes patient demographics and the etiology of encountered liver metastases.

2.2. Treatment planning: angiography and cone-beam CT

In a first step, in accordance with current guidelines [1], all patients underwent catheter angiography of the hepatic vasculature for treatment planning. All interventions were performed in a fully equipped angiography suite (ARTIS zeego and ARTIS pheno; Siemens Healthineers, Erlangen, Germany). In addition to standard digital subtraction angiography (DSA) CBCT was routinely performed.

All CBCT were standardized with an injection protocol of 36 mL 50/50 dilution of contrast media (Ultravist 370, 370 mg iodine/mL; Bayer Schering Pharma, Berlin, Germany) and sodium chloride 0.9 % at 2 mL/s with a 10 s scan delay. Injection was performed through a 2.7Fr microcatheter placed either in the proper hepatic artery, right or left hepatic artery as appropriate. A full 200 degree rotation took 7 s. A fixed tube voltage of 125 kV and a current-time-product of 345–360 mA s were used. Images were reconstructed with a slice width of 4 mm and an increment of 3 mm in axial and coronal plane.

After assessment of the hepatic vasculature anatomy coil embolization of all nonhepatic arterial flow was performed (especially gastroduodenal and right gastric artery) if required. Treatment was then simulated by injection of ^{99m}Tc-MAA through the microcatheter placed in the proper hepatic artery, left or right hepatic artery, respectively. Immediately after diagnostic angiography, single-photon emission CT was performed to evaluate for hepatopulmonary shunting and extrahepatic non-targed accumulation of ^{99m}Tc-MAA.

Table 1
Patient characteristics stratified by treatment response.

	All	SD/PR	PD	*p-value*
Total patients, n (%)	36 (100)	32 (88.9)	4 (11.1)	
Age (years), mean ± SD	61.1 ± 13	61.6 ± 12.8	57 ± 15.9	*0.510*
Male, n (%)	20 (55.6)	17	3	*0.406*
Female, n (%)	16 (44.4)	15	1	
Tumor entity				
Neuroendocrine tumor, n (%)	9 (25)	9	0	
Gastrointestinal tract, n (%)	7 (19.4)	7	0	
Melanoma, n (%)	5 (13.9)	5	0	
Pancreas, n (%)	3 (8.3)	3	0	
Mamma, n (%)	3 (8.3)	2	1	
Others, n (%)	9 (25)	6	3	
Pre-TARE treatment				
Chemotherapy, n (%)	30 (83.3)	27	3	*0.635*
Operation, n (%)	6 (16.7)	6	0	*0.343*
Radiotherapy, n (%)	3 (8.3)	3	0	*0.522*
Local intervention, n (%)	3 (8.3)	3	0	*0.522*
In-hospital outcome				
Complications, n (%)	4 (11.1)	3	1	*0.349*
In-hospital mortality, n (%)	0 (0)			
Follow-up period (months), mean ± SD	5.9 ± 0.8	5.9 ± 0.8	6.2 ± 0.9	*0.504*

SD = Stable disease; PR = Partial response; PD = Progressive disease.

2.3. Transarterial radioembolization

TARE was performed using ^{90}Y-microspheres (SIR-Spheres; SIRTeX Medical Limited, Lane Cove, Australia) administered into the appropriate hepatic artery as defined during diagnostic angiography. Dose calculation was done using the body surface area method [17].

2.4. Morphologic treatment response evaluation

Follow-up imaging consisted of CT (at least in portal venous phase) of the liver in 25 patients (69.4 %) and MR imaging with extracellular contrast agent (Dotarem®, Guerbet AG, Zurich, Switzerland) in 11 patients (30.6 %). Treatment response was evaluated according to RECIST version 1.1 [18]. A commercially available software was used to assess tumor progression (mint Lesion, Version 1.82; Mint Medical GmbH, Heidelberg, Germany).

First, three target metastases (104 metastases in total) were defined in pre-TARE CBCT in each patient. For all lesions, maximum diameter change between CBCT and post-TARE follow-up imaging at 6 months were recorded and response according to RECIST version 1.1 was calculated for each lesion independently. Complete response (CR), partial response (PR) and stable disease (SD) were defined as disease control. Progressive disease (PD) was defined as disease progression (Fig. 1).

2.5. Texture analysis

Texture features are derived from pre-treatment CBCT images by applying different filters to quantitatively assess these images. The image characterization is based on the pixel intensities within a region-

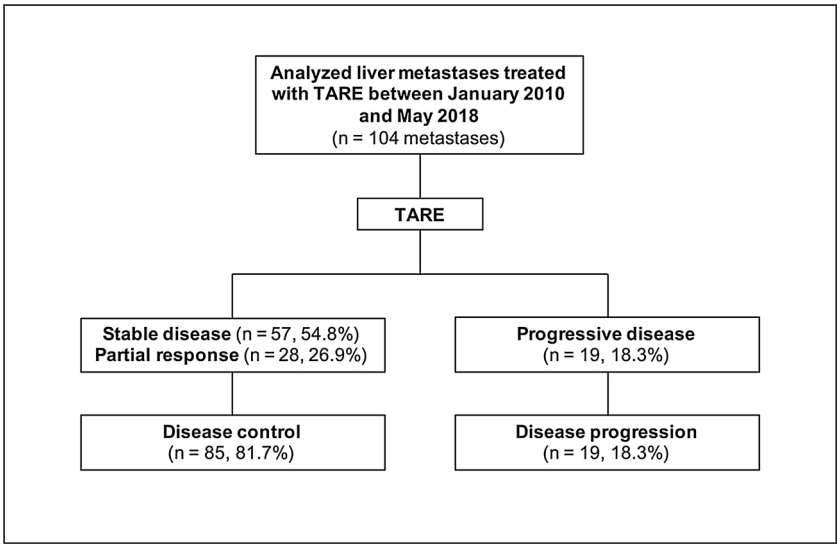

Fig. 1. Patient flow chart.

of-interest.

To do so, CBCT images were stored in the Digital Imaging and Communications in Medicine (DICOM) format. The images were post-processed with an in-house MATLAB routine, as described previously [19]. All images were subsequently loaded into the open-source software platform 3D Slicer with the *pyradiomics* extension [20].

Two readers (T.S. and M.M.; 1 and 6 years of experience in radiology, respectively) manually segmented the target lesions prior to treatment on axial slices. Intensity discretization was performed to a bin width of 25. Graylevel co-occurrence matrix (GLCM) features were computed at 4 inter-pixel distances. Then 104 radiomics features were extracted with the pyRadiomics package implemented into 3D Slicer. Most features are in accordance with those described in the Imaging Biomarker Standardization Initiative (IBSI). Radiomic features corresponded to seven different feature classes: First-order statistics/histogram matrix, shape-based features, gray-level co-occurrence matrix (GLCM), gray-level run length matrix (GLRLM), gray-level size zone matrix (GLSZM), neighboring gray tone difference matrix (NGTDM), and gray-level dependence matrix (GLDM) [21].

2.6. Dimension reduction

In order to reduce overfitting, dimension reduction was performed on the calculated texture analysis features (TA features). In a first instance, all texture features were normalized. Afterwards those TA features with decreased interrater-reproducibility, defined by an intraclass-correlation coefficient (ICC) of < 0.8 as previously shown [22], were discarded from further analysis.

2.7. Machine learning

For the outcome classification patients were dichotomized into a disease control (PR / SD) and disease progression (PD) group according to RECIST 1.1 [18]. Machine learning classifications were computed using open source software (WEKA, University of Waikato, Waikato, New Zealand). The classification task was performed on a training dataset of 83 metastases using a custom artificial neural network (ANN) based on Multilayer Perceptron with a batch size of 100, 2 hidden layers (nodes 5, 10), a learning rate of 0.4, a momentum of 0.22 and 4000 Epochs. The results were 10-fold cross-validated. The performance metrics of the ANN, performed on an unseen test dataset of 21 metastases, included sensitivity, specificity, precision, recall, F-measure, and the area-under-the-curve (AUC) from receiver operating characteristics (ROC) analysis.

Fig. 2 summarizes the process of texture analysis feature extraction and machine learning based outcome prediction.

2.8. Statistical analysis

For descriptive data mean values and standard deviations are provided. Continuous variables were compared using the independent two-sample *t*-test or Mann-Whitney test, respectively. Categorical variables were compared using the Chi-squared test. A two-tailed *p-value* of less than 0.05 was considered significant. Statistical analyses and plots were performed with a commercially available software (IBM, SPSS® Statistics v. 25, Chicago, IL).

3. Results

In total, 104 liver metastases of 36 patients (55.6 % male) were included for analysis. The mean size of liver metastases was 3.3 ± 2.2 cm in diameter.

Mean time interval between treatment planning and TARE was 18.4 $\pm$ 16.9 days. ^{90}Y-microspheres were administered through the proper hepatic artery in 15 patients (panhepatic 41.7 %), right hepatic artery in 18 patients (right lobe 50 %) and left hepatic artery in 3 patients (left lobe 8.3 %) with an average cumulative activity of 1.6 Gbq ($\pm$ 0.5 Gbq).

3.1. Response to TARE

At a mean follow-up of 5.9 ± 0.8 months, 57 (54.8 %) metastases showed stable disease, 28 (26.9 %) partial response and 19 (18.3 %) progressive disease. Accordingly, the disease control rate was 81.7 %. In-hospital mortality was 0%. Minor complications were observed in four patients (11.1 %): Mild rash after ^{90}Y-microspheres infusion, right upper quadrant pain, nausea, and access site hematoma. Fig. 3 shows examples of different treatment responses.

3.2. Dimension reduction

After dimension reduction 15 out of 104 (14.5 %) TA features remained for further analysis, depicted in Table 2. 14 out of 15 (93.3 %) TA features were derived from the GLCM.

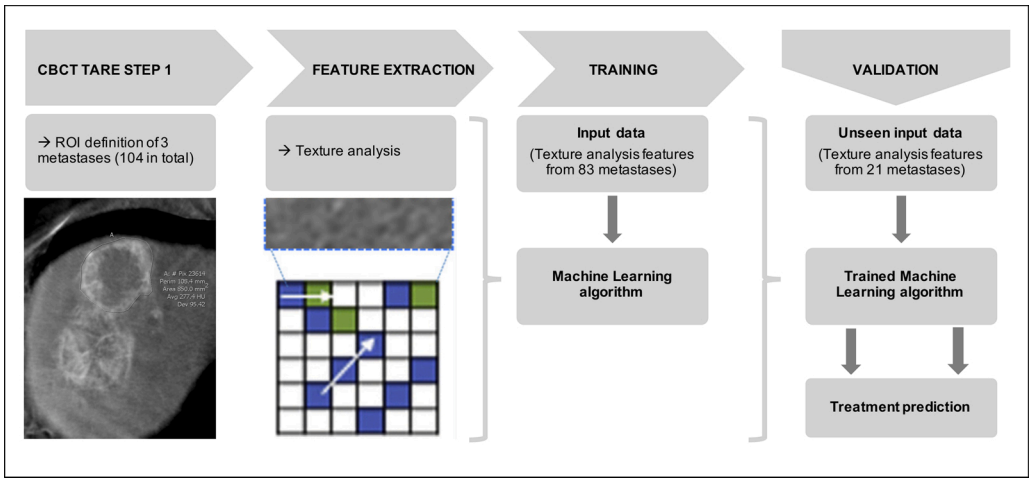

Fig. 2. Image post-processing flow chart for texture analysis based machine-learning to predict treatment response after transarterial radioembolization (TARE). On cone-beam CT (CBCT) images a region of interest is drawn around the selected metastases. Texture analysis features are extracted. The artificial neural network (ANN) is trained with the extracted texture analysis features of 83 liver metastases. Machine learning based prediction of tumor response after TARE on an unseen image set of 21 metastases is performed.

3.3. Prediction of liver metastases response to TARE

After 10-fold cross validation the Multilayer Perceptron ANN yielded a Sensitivity of 94.2 %, a Specificity of 67.7 %, a Precision of 0.8, a Recall of 0.84, an F-Measure of 0.81, and an AUC in ROC of 0.85 on the previously unseen test dataset of 21 metastases (Fig. 4).

4. Discussion

The present study indicates that machine learning based on selected texture analysis features could be a useful tool to predict treatment response based on pre-treatment CBCT images in patients with liver metastases undergoing transarterial radioembolization.

The herein used state of the art texture analysis tool is an open source software, developed to increase feature computation reliability and reproducibility. This tool has been used and validated in several radiomics studies across different imaging modalities and medical conditions [19,22].

Interestingly, after dimension reduction, 14 out of the 15 remaining texture analysis features used in the machine learning algorithm derived from the GLCM. The GLCM takes into account the spatial relationship of pixels. It characterizes the texture of an image by calculating how often pairs of pixels interconnected by a specified spatial relationship and specific values occur in an image. As part of this computational process, a matrix is calculated, from which statistical measures can then be extracted.

Similar to our approach, Park et al. [23] investigated texture analysis features on pre-treatment CT images in patients with hepatocellular carcinoma undergoing TACE. In treatment responders the hepatocellular carcinomas showed higher GLCM moments and lower homogeneity. The authors concluded that these features might reflect high tumor heterogeneity and most importantly the presence of intra-tumoral angiogenesis, which evidently renders tumors more susceptible to an intraarterial therapy such as TACE [23].

Other studies investigating the ability of texture analysis have found comparable results. In patients with hepatocellular carcinomas undergoing TACE texture analysis features were able to determine, which patient may benefit from surgery versus TACE or TACE alone versus TACE plus systemic chemotherapy [24,25]. However, these studies used different machine learning classifiers and strategies for dimension reduction.

For transarterial radioembolization there is only one radiomics study by Mosconi et al. [16] where texture analysis features were analyzed on pre-treatment CT images to predict treatment response. However, the study only included patients with intrahepatic cholangiocarcinoma. In treatment responders the intrahepatic cholangiocarcinomas showed higher mean histogram values, corresponding to higher contrast uptake in the arterial phase, and a more homogeneous distribution. More precisely, lower kurtosis, GLCM contrast, GLCM dissimilarity and higher GLCM homogeneity and GLCM correlation were found.

In the early days of texture analysis, due to inherent image noise of CT images, there were concerns that the extracted texture features might only reflect image noise instead of true biological heterogeneity of the tumor. This problem was overcome with image filtration techniques that are able to reduce image noise [8]. In our study we decided to use cone-beam CT images from the treatment planning procedure prior to TARE as the pre-TARE imaging workup was extremely heterogeneous between patients. Specifically, most patients were referred from external hospitals specifically for the procedure and thus, some had initially received MRI workup, while others had undergone CT scans, often from various vendors and with various scanning protocols. In contrast, CBCTs were performed in a standardized manner with identical reconstruction protocols, which made them comparable between all patients over a long period-of-time. In general, CBCT images provide higher spatial resolution with reduced contrast resolution compared to multidetector CT images [26]. Nevertheless, they are susceptible to movement artifacts and exhibit higher image noise which could be problematic for texture analysis. Two previous studies on non-small cell lung cancer patients have however shown that texture analysis on CBCT images is robust and reproducible [27,28].

As texture analysis features are abstract numbers and thus difficult to implement into standard image interpretation artificial intelligence could be used to close the gap between overwhelming imaging data and decision making in oncologic patients. More precisely, the extracted texture analysis features showing differences between responders and non-responders could be used for supervised machine learning. Specifically, an artificial neural network initially trained on the extracted texture analysis features and the corresponding treatment response could then be used for outcome prediction on new data sets [29–31].

To our knowledge this is the first study to investigate the potential of texture analysis based machine learning on pre-treatment imaging of patients with liver metastases undergoing TARE. Our model achieved a good accuracy for differentiating disease control (PR / SD) from disease progression (PD) with a sensitivity of 94.2 %, a specificity of 67.7 % and an AUC in ROC of 0.85 (Fig. 4).

Few studies in interventional oncology have yet investigated the ability of machine learning to predict tumor response or survival with most studies focusing on patients with hepatocellular carcinoma undergoing TACE [12–15].

Abajian et al. [13] trained an ANN with clinical data, pre-treatment imaging patterns (relative tumor signal intensity and number of tumors) and therapeutic features (conventional TACE or not and systemic

Fig. 3. Examples of metastases in pre-treatment cone-beam CT (left column) and follow-up computed tomography scans after transarterial radioembolization (right column). All encountered treatment responses according to RECIST 1.1. are illustrated: "partial response" (first row), "stable disease" (second row) and "progressive disease" (third row). Pre-treatment metastases are labeled by white arrows, post-TARE metastases by white dotted arrows and newly appeared metastases by white stars.

chemotherapy or not) rather than with texture analysis features. This ANN yielded a sensitivity and specificity of 62.5 % and 82.1 %, respectively for treatment response prediction. A similar approach was used by Mähringer et al. [14] who trained the ANN with clinical, laboratory and imaging parameters which are used in current risk scores to predict 1-year survival after TACE. With an AUC of 0.77, this ANN performed better than traditional scoring systems in predicting 1-year survival after TACE.

Only Morshid et al. [12] chose a texture analysis based approach for pre-TACE CT images in combination with BCLC stage thereby achieving an accuracy rate for response prediction of 74.2 %. These studies suggest that it might be useful to add clinical parameters to the texture analysis features in an effort to further improve the accuracy of the machine learning algorithm.

Table 2
Texture analysis features remaining after dimension reduction.

#	TA feature
1	MorMzNo
2	YD5GlcmN3SumOfSqs
3	YD5GlcmN3SumAverg
4	YD5GlcmN3SumVarnc
5	YD5GlcmN3SumEntrp
6	YD5GlcmN3Entropy
7	YD5GlcmN3DifVarnc
8	YD5GlcmN3InvDfMom
9	YD5GlcmN3Correlat
10	YD5GlcmN3Area
11	YD5GlcmN3Contrast
12	YD5GlcmN2Entropy
13	YD5GlcmN2DifVarnc
14	YD5GlcmN2DifEntrp
15	YD5GlcmN3Area

TA = Texture analysis.

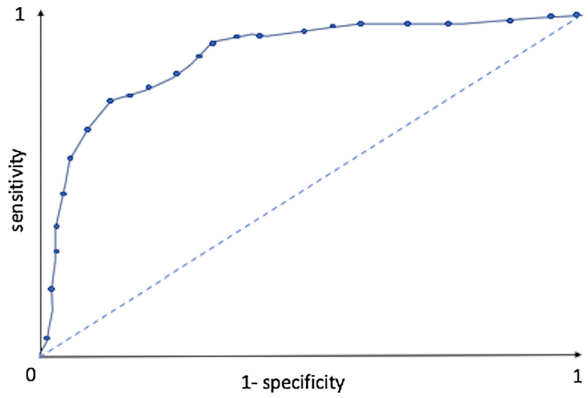

Fig. 4. ROC curve of the Multilayer Perceptron ANN on a previously unseen test data of 21 liver metastases (AUC, 0.85).
ANN, artificial neuronal network; AUC, area under the curve; ROC, receiver operating characteristic curve.

Supported by our results, all published studies investigating machine learning based outcome prediction on pre-treatment images so far reason that ANNs may help to identify patients who will benefit from interventional oncologic treatments. Ultimately, this may result in better patient selection and avoid unnecessary treatments. Furthermore, it may be possible to detect metastases within a patient that are potentially less responsive to TARE. These identified metastases could be treated with combined minimally invasive therapies, namely additional percutaneous thermoablative procedures. Further studies have to be conducted to validate these assumptions.

There are major limitations we must acknowledge. First, we analyzed a highly heterogeneous patient population with liver metastases from different primaries. Second, the sample size of 36 patients is fairly small. This limitation was overcome by analyzing multiple metastases per patient, resulting in 104 analyzed metastases. However, this carries the risk of biasing the results as no external validation was performed. Furthermore, with a disease control rate of 81.7 % there was a disequilibrium in the training set, as only few cases of disease progression were available to train the ANN. Finally, it must be emphasized that due to the small number of patients and heterogeneous tumor entities, ultimately no conclusions can be drawn that allow generalizable results between tumor entities.

In conclusion, our study indicates that texture analysis-based machine learning may has potential to predict treatment response to TARE using pre-treatment CBCT images of patients with liver metastases with high accuracy.

Funding sources

This research did not receive any specific grant from funding agencies in the public, commercial, or not-for-profit sectors.

Ethics statement

This retrospective study was approved by the local Ethics Committee and conducted according to the principles of the Declaration of Helsinki. Written informed consent requirement was waived.

CRediT authorship contribution statement

Adrian Kobe: Conceptualization, Data curation, Investigation, Methodology, Software, Visualization, Writing - original draft, Writing - review & editing. **Juliana Zgraggen:** Data curation, Investigation, Visualization, Writing - original draft, Writing - review & editing. **Florian Messmer:** Data curation, Investigation, Writing - original draft, Writing - review & editing. **Gilbert Puippe:** Data curation, Investigation, Writing - original draft, Writing - review & editing. **Thomas Sartoretti:** Data curation, Investigation, Writing - original draft, Writing - review & editing. **Hatem Alkadhi:** Data curation, Investigation, Writing - original draft, Writing - review & editing. **Thomas Pfammatter:** Conceptualization, Investigation, Methodology, Project administration, Resources, Software, Supervision, Validation, Writing - original draft, Writing - review & editing. **Manoj Mannil:** Conceptualization, Data curation, Formal analysis, Investigation, Methodology, Software, Supervision, Validation, Visualization, Writing - original draft, Writing - review & editing.

Declaration of Competing Interest

The authors report no declarations of interest.

References

[1] S.A. Padia, R.J. Lewandowski, G.E. Johnson, D.Y. Sze, T.J. Ward, R.C. Gaba, M. O. Baerlocher, V.L. Gates, A. Riaz, D.B. Brown, N.H. Siddiqi, T.G. Walker, J. E. Silberzweig, J.W. Mitchell, B. Nikolic, R. Salem, S. of I.R.S. of P. Committee, Radioembolization of hepatic malignancies: background, quality improvement guidelines, and future directions, J. Vasc. Interv. Radiol. 28 (2017) 1–15, https://doi.org/10.1016/j.jvir.2016.09.024.

[2] R. Salem, K.G. Thurston, Radioembolization with 90Yttrium Microspheres: A State-of-the-Art Brachytherapy Treatment for Primary and Secondary Liver Malignancies. Part 1: Technical and methodologic considerations, J. Vasc. Interv. Radiol. 17 (2006) 1251–1278, https://doi.org/10.1097/01.rvi.0000233785.75257.9a.

[3] F. Morsbach, T. Pfammatter, C.S. Reiner, M.A. Fischer, B.-R. Sah, S. Winklhofer, E. Klotz, T. Frauenfelder, A. Knuth, B. Seifert, N. Schaefer, H. Alkadhi, Computed tomographic perfusion imaging for the prediction of response and survival to transarterial radioembolization of liver metastases, Invest. Radiol. 48 (2013) 787–794, https://doi.org/10.1097/rli.0b013e31829810f7.

[4] F. Morsbach, B.-R. Sah, L. Spring, G. Puippe, S. Gordic, B. Seifert, N. Schaefer, T. Pfammatter, H. Alkadhi, C.S. Reiner, Perfusion CT best predicts outcome after radioembolization of liver metastases: a comparison of radionuclide and CT imaging techniques, Eur. Radiol. 24 (2014) 1455–1465, https://doi.org/10.1007/s00330-014-3180-3.

[5] K.T. Sato, R.A. Omary, C. Takehana, S. Ibrahim, R.J. Lewandowski, R.K. Ryu, R. Salem, The role of tumor vascularity in predicting survival after yttrium-90 radioembolization for liver metastases, J. Vasc. Interv. Radiol. 20 (2009) 1564–1569, https://doi.org/10.1016/j.jvir.2009.08.013.

[6] E. Garin, L. Lenoir, Y. Rolland, J. Edeline, H. Mesbah, S. Laffont, P. Porée, B. Clément, J.-L. Raoul, E. Boucher, Dosimetry based on 99mTc-macroaggregated albumin SPECT/CT accurately predicts tumor response and survival in hepatocellular carcinoma patients treated with 90Y-loaded glass microspheres: preliminary results, J Nucl Medicine Official Publ Soc Nucl Medicine. 53 (2012) 255–263, https://doi.org/10.2967/jnumed.111.094235.

[7] A. Dhabuwala, P. Lamerton, R.S. Stubbs, Relationship of 99mtechnetium labelled macroaggregated albumin (99mTc-MAA) uptake by colorectal liver metastases to response following Selective Internal Radiation Therapy (SIRT), Bmc Nucl Medicine. 5 (2005) 7, https://doi.org/10.1186/1471-2385-5-7.

[8] M.G. Lubner, A.D. Smith, K. Sandrasegaran, D.V. Sahani, P.J. Pickhardt, CT texture analysis: definitions, applications, biologic correlates, and challenges, Radiographics. 37 (2017) 1483–1503, https://doi.org/10.1148/rg.2017170056.

[9] N. Horvat, H. Veeraraghavan, M. Khan, I. Blazic, J. Zheng, M. Capanu, E. Sala, J. Garcia-Aguilar, M.J. Gollub, I. Petkovska, MR imaging of rectal Cancer: radiomics analysis to assess treatment response after neoadjuvant therapy, Radiology. 287 (2018) 833–843, https://doi.org/10.1148/radiol.2018172300.
[10] G.-W. Ji, Y.-D. Zhang, H. Zhang, F.-P. Zhu, K. Wang, Y.-X. Xia, Y.-D. Zhang, W.-J. Jiang, X.-C. Li, X.-H. Wang, Biliary tract Cancer at CT: a radiomics-based model to predict lymph node metastasis and survival outcomes, Radiology. 290 (2019) 90–98, https://doi.org/10.1148/radiol.2018181408.
[11] H. Wang, B. Song, N. Ye, J. Ren, X. Sun, Z. Dai, Y. Zhang, B.T. Chen, Machine learning-based multiparametric MRI radiomics for predicting the aggressiveness of papillary thyroid carcinoma, Eur. J. Radiol. 122 (2020), 108755, https://doi.org/10.1016/j.ejrad.2019.108755.
[12] A. Morshid, K.M. Elsayes, A.M. Khalaf, M.M. Elmohr, J. Yu, A.O. Kaseb, M. Hassan, A. Mahvash, Z. Wang, J.D. Hazle, D. Fuentes, A machine learning model to predict hepatocellular carcinoma response to transcatheter arterial chemoembolization, Radiology Artif Intell. 1 (2019), e180021, https://doi.org/10.1148/ryai.2019180021.
[13] A. Abajian, N. Murali, L.J. Savic, F.M. Laage-Gaupp, N. Nezami, J.S. Duncan, T. Schlachter, M. Lin, J.-F. Geschwind, J. Chapiro, Predicting treatment response to intra-arterial therapies for hepatocellular carcinoma with the use of supervised machine learning-an artificial intelligence concept, J. Vasc. Interv. Radiol. 29 (2018) 850–857, https://doi.org/10.1016/j.jvir.2018.01.769, e1.
[14] A. Mähringer-Kunz, F. Wagner, F. Hahn, A. Weinmann, S. Brodehl, S. Schotten, J. B. Hinrichs, C. Düber, P.R. Galle, D.P. Dos Santos, R. Kloeckner, Predicting survival after transarterial chemoembolization for hepatocellular carcinoma using a neural network: a Pilot Study, Liver Int. 40 (2020) 694–703, https://doi.org/10.1111/liv.14380.
[15] J. Peng, S. Kang, Z. Ning, H. Deng, J. Shen, Y. Xu, J. Zhang, W. Zhao, X. Li, W. Gong, J. Huang, L. Liu, Residual convolutional neural network for predicting response of transarterial chemoembolization in hepatocellular carcinoma from CT imaging, Eur. Radiol. 30 (2019) 413–424, https://doi.org/10.1007/s00330-019-06318-1.
[16] C. Mosconi, A. Cucchetti, A. Bruno, A. Cappelli, I. Bargellini, C.D. Benedittis, G. Lorenzoni, A. Gramenzi, F.P. Tarantino, L. Parini, V. Pettinato, F. Modestino, G. Peta, R. Cioni, R. Golfieri, Radiomics of cholangiocarcinoma on pretreatment CT can identify patients who would best respond to radioembolisation, Eur. Radiol. (2020) 1–11, https://doi.org/10.1007/s00330-020-06795-9.
[17] W.-Y. Lau, A.S. Kennedy, Y.H. Kim, H.K. Lai, R.-C. Lee, T.W.T. Leung, C.-S. Liu, R. Salem, B. Sangro, B. Shuter, S.-C. Wang, Patient selection and activity planning guide for selective internal radiotherapy with Yttrium-90 resin microspheres, Int J Radiat Oncol Biology Phys. 82 (2012) 401–407, https://doi.org/10.1016/j.ijrobp.2010.08.015.
[18] E.A. Eisenhauer, P. Therasse, J. Bogaerts, L.H. Schwartz, D. Sargent, R. Ford, J. Dancey, S. Arbuck, S. Gwyther, M. Mooney, L. Rubinstein, L. Shankar, L. Dodd, R. Kaplan, D. Lacombe, J. Verweij, New response evaluation criteria in solid tumours: revised RECIST guideline (version 1.1), Eur. J. Cancer 1990 (45) (2009) 228–247, https://doi.org/10.1016/j.ejca.2008.10.026.
[19] M. Mannil, J. von Spiczak, R. Manka, H. Alkadhi, Texture analysis and machine learning for detecting myocardial infarction in Noncontrast low-dose computed tomography: unveiling the invisible, Invest. Radiol. 53 (2018) 338–343, https://doi.org/10.1097/rli.0000000000000448.
[20] J.J.M. van Griethuysen, A. Fedorov, C. Parmar, A. Hosny, N. Aucoin, V. Narayan, R.G.H. Beets-Tan, J.-C. Fillion-Robin, S. Pieper, H.J.W.L. Aerts, Computational radiomics system to decode the radiographic phenotype, Cancer Res. 77 (2017) e104–e107, https://doi.org/10.1158/0008-5472.can-17-0339.
[21] B. Baessler, T. Nestler, D.P.D. Santos, P. Paffenholz, V. Zeuch, D. Pfister, D. Maintz, A. Heidenreich, Radiomics allows for detection of benign and malignant histopathology in patients with metastatic testicular germ cell tumors prior to post-chemotherapy retroperitoneal lymph node dissection, Eur. Radiol. 30 (2019) 2334–2345, https://doi.org/10.1007/s00330-019-06495-z.
[22] P. Kambakamba, M. Mannil, P.E. Herrera, P.C. Müller, C. Kuemmerli, M. Linecker, J. von Spiczak, M.W. Hüllner, D.A. Raptis, H. Petrowsky, P.-A. Clavien, H. Alkadhi, The potential of machine learning to predict postoperative pancreatic fistula based on preoperative, non-contrast-enhanced CT: a proof-of-principle study, Surgery. 167 (2019) 448–454, https://doi.org/10.1016/j.surg.2019.09.019.
[23] H.J. Park, J.H. Kim, S.-Y. Choi, E.S. Lee, S.J. Park, J.Y. Byun, B.I. Choi, Prediction of therapeutic response of hepatocellular carcinoma to transcatheter arterial chemoembolization based on pretherapeutic dynamic CT and textural findings, AJR Am. J. Roentgenol. 209 (2017) W211–W220, https://doi.org/10.2214/ajr.16.17398.
[24] M. Li, S. Fu, Y. Zhu, Z. Liu, S. Chen, L. Lu, C. Liang, Computed tomography texture analysis to facilitate therapeutic decision making in hepatocellular carcinoma, Oncotarget 7 (2016) 13248–13259, https://doi.org/10.18632/oncotarget.7467.
[25] S. Fu, S. Chen, C. Liang, Z. Liu, Y. Zhu, Y. Li, L. Lu, Texture analysis of intermediate-advanced hepatocellular carcinoma: prognosis and patients' selection of transcatheter arterial chemoembolization and sorafenib, Oncotarget 8 (2016), https://doi.org/10.18632/oncotarget.13675.
[26] R. Gupta, A.C. Cheung, S.H. Bartling, J. Lisauskas, M. Grasruck, C. Leidecker, B. Schmidt, T. Flohr, T.J. Brady, Flat-panel volume CT: fundamental principles, technology, and applications, Radiographics Rev Publ Radiological Soc North Am Inc. 28 (2008) 2009–2022, https://doi.org/10.1148/rg.287085004.
[27] J.E. van Timmeren, R.T.H. Leijenaar, W. van Elmpt, B. Reymen, C. Oberije, R. Monshouwer, J. Bussink, C. Brink, O. Hansen, P. Lambin, Survival prediction of non-small cell lung cancer patients using radiomics analyses of cone-beam CT images, Radiotherapy Oncol. J. European Soc. Ther Radiology Oncol. 123 (2017) 363–369, https://doi.org/10.1016/j.radonc.2017.04.016.
[28] X. Fave, D. Mackin, J. Yang, J. Zhang, D. Fried, P. Balter, D. Followill, D. Gomez, A. K. Jones, F. Stingo, J. Fontenot, L. Court, Can radiomics features be reproducibly measured from CBCT images for patients with non-small cell lung cancer? Med. Phys. 42 (2015) 6784–6797, https://doi.org/10.1118/1.4934826.
[29] I. Sinha, D.P. Aluthge, E.S. Chen, I.N. Sarkar, S.H. Ahn, Machine learning offers exciting potential for predicting postprocedural outcomes: a framework for developing random forest models in IR, J. Vasc. Interv. Radiol. 31 (2020) 1018–1024, https://doi.org/10.1016/j.jvir.2019.11.030, e4.
[30] J. Song, Y. Yin, H. Wang, Z. Chang, Z. Liu, L. Cui, A review of original articles published in the emerging field of radiomics, Eur. J. Radiol. 127 (2020), 108991, https://doi.org/10.1016/j.ejrad.2020.108991.
[31] L. Saba, M. Biswas, V. Kuppili, E.C. Godia, H.S. Suri, D.R. Edla, T. Omerzu, J. R. Laird, N.N. Khanna, S. Mavrogeni, A. Protogerou, P.P. Sfikakis, V. Viswanathan, G.D. Kitas, A. Nicolaides, A. Gupta, J.S. Suri, The present and future of deep learning in radiology, Eur. J. Radiol. 114 (2019) 14–24, https://doi.org/10.1016/j.ejrad.2019.02.038.